Study on the removal capability of trinitrotoluene in water using the UV/WO_3/H_2O_2 photo oxidation method

Dinh Trong Nghia[1*], Vu Thi Mai[2], Phi Hoang Thuy Quynh[1], Doan Cong Danh[1]

[1]Institute of Materials, Biology and Environment, Academy of Military Science and Technology, 17 Hoang Sam, Nghia Do, Hanoi, Vietnam;
[2]Hanoi University of Natural Resources and Environment, 41A Phu Dien, Phu Dien, Hanoi, Vietnam.
[*]Corresponding author: TrongnghiaCNM2020@gmail.com
Received 10 Aug. 2025; Revised 8 Sep. 2025; Accepted 20 Sep. 2025; Published 2 Oct. 2025.
DOI: https://doi.org/10.54939/1859-1043.j.mst.106.2025.94-101

ABSTRACT

The paper presents the results of synthesizing WO_3 by the chemical precipitation method, along with an evaluation of its physicochemical properties, morphology, crystal structure, and chemical characteristics. In addition, preliminary results are introduced regarding the removal efficiency of TNT from aqueous solution by photocatalytic oxidation, in which •OH and h^+ play the main role as oxidizing species. The results indicate that the synthesized WO_3 possesses a hexagonal crystal structure, a density of 7.920 g/cm³, an absorption intensity of 1.45 a.u at a wavelength of λ = 285 nm, and a band gap energy of approximately 3.3 eV. The protonation process favors the widening of the energy band gap and enhances the oxidation potential of WO_3, thereby improving its photocatalytic performance and increasing its ability to absorb UVB light. The UV/WO_3/H_2O_2 photocatalytic oxidation process, with a fixed H_2O_2 concentration of 2.94 × 10^{-3} M, an optimal catalyst dosage of 300 mg WO_3, and a UV lamp power of 10 W, achieved a TNT removal efficiency of 98.7% at an initial concentration of 100 mg/L after 60 minutes of reaction under ambient temperature.

Keywords: Tungsten trioxide; Photo-oxidation; Trinitrotoluene; Treatment.

1. INTRODUCTION

2,4,6-Trinitrotoluene (TNT) is one of the widely used nitroaromatic compounds in various military activities and defense manufacturing [1]. Due to its high toxicity, persistence, limited biodegradability, and tendency to accumulate in the environment, TNT has a negative impact on both ecosystems and human health [2]. Biological wastewater treatment methods have proven ineffective in treating wastewater containing TNT. This is mainly because the nitro groups in TNT interfere with the activity of enzymes involved in the biodegradation process [3]. Various methods for the treatment of TNT have been reported, including: adsorption using activated carbon, oxidation with hydrogen peroxide/ozone, supercritical water oxidation, Fenton oxidation and photocatalytic oxidation [4,9]. Each method has its own advantages and limitations. For example, in the case of activated carbon, its main advantage lies in its high adsorption capacity due to its well-developed porous structure, which allows it to effectively adsorb organic molecules. Despite its effectiveness and low cost, activated carbon treatment provides only a temporary solution rather than complete removal. In addition, advanced oxidation processes (AOPs) have demonstrated high efficiency in degrading persistent organic compounds. They also face certain limitations due to the requirement for additional chemicals and specific operational conditions, which significantly increase the treatment cost [4].

Photocatalytic oxidation has attracted growing interest in the field of wastewater treatment due to its high efficiency in degrading organic pollutants and its ability to operate effectively at low temperature and pressure conditions [6-9]. Several photocatalytic materials have been extensively studied, notably ZnO and SnO_2, due to their effective e^-–h^+ pair generation, relatively good stability, and low synthesis cost. ZnO tends to dissolve in acidic environments, which causes

structural degradation and reduced photocatalytic performance over time. SnO_2, while more stable than ZnO, is still not fully resistant under low pH conditions, and its photocatalytic efficiency is generally lower compared to other materials due to the high recombination rate of electron-hole pairs [6]. Recently, WO_3 has attracted considerable research interest due to its unique physicochemical properties, such as electrochromism, photochromism, and photocatalysis. WO_3 is a photocatalyst capable of effectively absorbing UV light and generating reactive oxygen species such as $\bullet OH$, $\bullet O_2^-$, which can degrade persistent organic pollutants like TNT [7]. In addition, WO_3 exhibits high stability, is non-toxic, and can operate effectively over a wide pH range; it is suitable for TNT wastewater treatment [8].

To further contribute to the aforementioned research direction, particularly in the field of TNT wastewater treatment, this study presents the synthesis and thorough characterization of WO_3-based photocatalysts, including their physicochemical properties, morphology, chemical composition, and characteristic bonding features. Specifically, this study investigates the efficiency of TNT removal from water using a WO_3/H_2O_2/UV photocatalytic system, an advanced oxidation process AOPs that simultaneously employs WO_3 as the photocatalyst, H_2O_2 as the oxidizing agent, and UV light as the photon source. In this system, WO_3 acts as the UV–UV-absorbing material to excite electrons, while H_2O_2 functions as an electron acceptor and participates in generating highly reactive hydroxyl radicals, which are capable of breaking down the stable molecular structure of TNT.

2. MATERIALS AND METHODS

2.1. Chemicals and equipment

2.1.1. Chemicals

Trinitrotoluene ($C_7H_5N_3O_6$) in crystalline form with pA-grade purity (Vietnam); Tert-butanol ($C_4H_{10}O$) (99%), ethanol (C_2H_5OH) (95%), hydrogen peroxide (H_2O_2) with a stock solution concentration of 30% (w/v), sodium tungstate dihydrate ($Na_2WO_4.2H_2O$) (99.5%), hydrochloric acid (HCl) (37%), and sodium bicarbonate ($NaHCO_3$) (99%) were all of analytical grade (PA), supplied by S.I Analytics, China.

2.1.2. Equipment

FE-SEM Hitachi S-4800, Japan; UV-Vis DRS spectroscopy, Jasco International, Japan; D8 Advance, Bruker, Germany; FT-IR Nicolet iS10, Thermo Scientific, USA; COD HI839800-02, Hanna Instruments, USA; LC-QTOF-MS, SCIEX X500R, USA; magnetic stirrer Vera, Cole Parmer, USA; UV lamp, Philips, China; and other available instruments and equipment from the Institute of Biomaterials and Environment.

2.2. Research methods

2.2.1. Research on evaluating some properties, morphology, characteristic bonding, crystal structure, and radiation absorption capacity of WO_3

The surface morphology and elemental composition of WO_3 were characterized using a field emission scanning electron microscope and equipped with energy-dispersive X-ray spectroscopy, model Hitachi S-4800, Japan; the chemical bonding characteristics of the synthesized material were identified by FT-IR spectroscopy using the FT-IR Nicolet iS10, Thermo Scientific, USA; the radiation absorption capacity was measured using UV-Vis DRS spectroscopy with the UV-Vis DRS spectroscopy, Jasco International, Japan; the instruments is from the Institute of Materials Science, Vietnam Academy of Science and Technology.

The crystal structure of WO_3 was determined by X-ray diffraction using the D8 Advance, Bruker, Germany, from the Institute of Chemistry, Vietnam Academy of Science and Technology.

2.2.2. Analytical method for TNT determination

TNT concentration was determined using a liquid chromatography quadrupole time-of-flight mass spectrometer (LC-QTOF-MS, SCIEX X500R, USA) equipped with a Turbo V™ source and an APCI ionization source. Chromatographic separation was carried out on a Gemini C18 110 Å column (2.0 mm × 50 mm × 3 µm, Phenomenex, USA) with a binary pump and column oven. The mobile phase consisted of (A) water with 0.1% formic acid and (B) methanol with 0.1% formic acid, with the following gradient program: 10% B (0–1 min) → 90% B (1–3 min) → 90% B (3–6 min) → 10% B (6–8 min). The flow rate was set at 0.3 mL/min.

Mass spectrometric detection was performed under the following conditions: curtain gas 25 psi, nebulizer current −3 µA, gas pressure 50 psi, source temperature 500 °C, entrance potential −80 V, and collision energy −10 V. Multiple reaction monitoring (MRM) mode was employed. TNT was detected at a retention time of 3.591 min with a precursor ion of m/z 226.01 ($[M–H]^-$) and two fragment ions at m/z 45.9923 and 76.0178. Calibration curves were established over the concentration range of 1–150 µg/L, with limits of detection (LOD) and quantification (LOQ) of 0.202 µg/L and 0.637 µg/L, respectively, and a correlation coefficient (R^2) of 0.9995.

2.2.3. Study on the ability to treat TNT in water using the UV/WO_3/H_2O_2 method

To investigate the photocatalytic degradation of TNT, 100 mg of TNT was accurately weighed into a beaker containing 1000 mL of deionized water and stirred on a magnetic stirrer for 12 hours to ensure complete dispersion. The catalyst was then added in varying amounts depending on the experimental design: (i) 200 mg for the comparison of TNT degradation efficiency in different systems (WO_3/UV, UV/H_2O_2, and WO_3/UV/H_2O_2), (ii) 100, 200, 300, 400, and 500 mg for evaluating the effect of WO_3 concentration, and (iii) 300 mg for reactive species determination (based on the optimal dosage identified in section ii). After catalyst addition, the suspensions were stirred in the dark for 2 hours to establish adsorption–desorption equilibrium, followed by centrifugation to collect the supernatant for the initial concentration measurement (C_0). Photodegradation experiments were conducted under identical conditions: pH from 4-5, UV irradiation (λ = 285 nm, W = 10 W), H_2O_2 concentration of 2.94×10^{-3} M. To assess the effect of reactive species, TBA 10 mM and sodium bicarbonate $NaHCO_3$ 4.76 M were separately introduced in control runs. At predetermined time intervals (15, 30, 45, 60, 75, 90, 105, and 120 minutes), samples were withdrawn, centrifuged, and the clarified supernatants were analyzed to determine the residual TNT concentration (C_t). The TNT removal efficiency (H, %) was calculated using equation (1):

$$H\% = \frac{C_0 - C_t}{C_0} \times 100\ (\%) \quad (1)$$

Where: H represents the degradation efficiency, while C_0 and C_t denote the concentrations of TNT at the initial time and at time t, respectively, expressed in mg/L.

3. RESULTS AND DISCUSSION

3.1. Results of evaluating the properties, morphology, characteristic bonding, crystal structure, and radiation absorption capacity of WO_3

The FE-SEM analysis results of WO_3 material are presented in figure 1. The FE-SEM images reveal that the WO_3 material consists of sheet-like nanoparticles with relatively uniform size distribution.

The crystal structure of the WO_3 material was identified by X-ray diffraction (XRD), and the results are presented in figure 2. The XRD pattern of WO_3 shows three strong and sharp diffraction peaks at 2θ = 14.06°, 23.24°, 28.23°, corresponding to the (010), (001), (200) crystal planes, respectively. Additional low-intensity peaks are observed at 2θ = 36.81°, 49.82°, 55.66°, which correspond to the (110), (011), (200) planes. These diffraction peaks are characteristic of the hexagonal phase of WO_3, which belongs to the P63/mcm (No. 193) space group, in accordance

with the standard (JCPDS card No. 01-075-2187) [11, 12]. Thus, the X-ray diffraction analysis confirmed the presence of characteristic diffraction peaks corresponding to WO_3 synthesized via the chemical precipitation method.

The FTIR spectrum of the synthesized WO_3 sample exhibits distinct vibrational features characteristic of tungsten oxide. The broad and intense absorption centered around 805.63 cm^{-1} corresponds to terminal asymmetric W=O stretching, while the band at 611.30 cm^{-1} is attributed to bridging W–O–W bonds within the WO_6 octahedral framework. Additionally, the presence of multiple overlapped peaks in the 400–500 cm^{-1} region suggests lattice distortions or oxygen vacancies. These characteristics may originate from the strong protonation process using 1 M HCl, with a molar ratio of H^+:W = 220, which promotes the extensive formation of terminal W=O double bonds and facilitates the precipitation and formation of a WO_3 lattice containing oxygen vacancies [11].

The radiation absorption capability of the synthesized WO_3 material was evaluated using UV-Vis diffuse reflectance spectroscopy (UV-Vis DRS), with a scan wavelength range from 200 nm to 1400 nm, a scan rate of 400 nm/min, and a D_2/WI light source (figure 4). In the short-wavelength region (200 – 420 nm), strong absorption peaks were observed, which are attributed to intense electronic transitions, with absorption intensities reaching approximately 1.45 a.u.

Additionally, the band gap energy E_g of the WO_3 was determined to be approximately 3.3 eV, using the Kubelka–Munk function as calculated from the equation. This was achieved by extrapolating the linear portion of the plot of $(F(R_\infty).h\nu)^{1/\gamma}$ versus hν, which enables the estimation of the optical band gap [12]. This value is higher than that of conventional WO_3 (2.6–2.9 eV), indicating a more positive valence band potential +3.4 V (vs. NHE), surface protonation markedly enhances the photocatalytic activity of WO_3 [7].

Thus, based on the radiation absorption spectrum and the band gap value determined using the Kubelka–Munk function, it can be concluded that WO_3 exhibits strong absorption in the ultraviolet region. These characteristics and properties are consistent with those reported in previous studies [12, 13, 15].

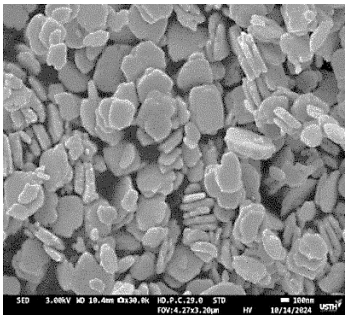

Figure 1. *FE-SEM analysis of WO_3.*

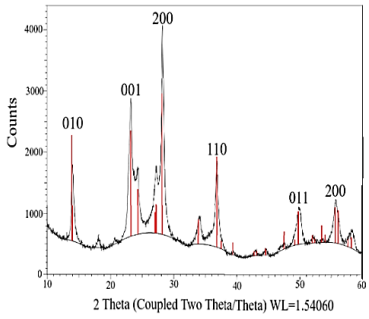

Figure 2. *X-ray diffraction (XRD) pattern of WO_3.*

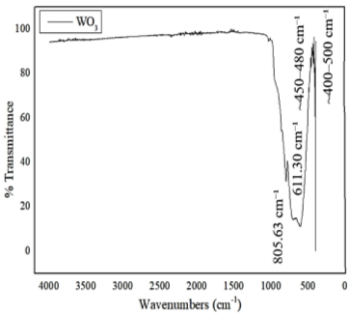

Figure 3. *FTIR spectrum of WO_3.*

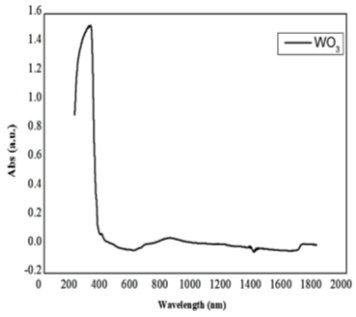

Figure 4. *UV-Vis DRS spectrum of WO_3.*

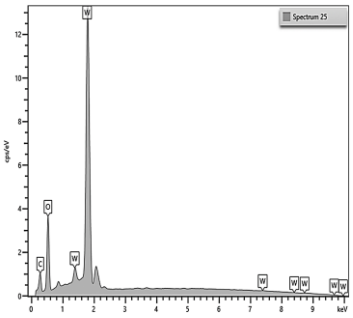

Figure 5. *EDX spectrum of WO_3.*

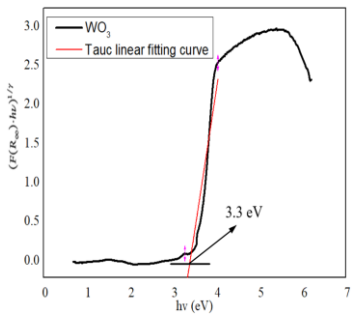

Figure 6. *Energy band gap of WO_3.*

The X-ray energy dispersive spectroscopy results of the WO_3 sample shown in figure 5 indicate the presence of characteristic diffraction peaks for W at energy levels of 1.40, 1.92, 7.43, 8.45, and 9.64 keV. The characteristic diffraction peak for O appears at an energy level of 0.51 keV [14]. This indicates that the synthesized WO_3 material was successful, with the complete presence of all constituent elements and no foreign elements detected.

3.2. Results of the study on the ability to treat TNT in water using the UV/WO_3/H_2O_2 method

In this study, a TNT solution concentration of 100 mg/L was selected for the photocatalytic degradation experiments to evaluate the treatment performance of the UV/WO_3/H_2O_2 system. The results of TNT degradation efficiency are presented in figure 6. In the absence of H_2O_2, the WO_3 material achieved a TNT removal efficiency of 20.8% after 120 minutes. This can be explained by the fact that upon UV irradiation, WO_3 is photoactivated, leading to the generation of e^-–h^+ pairs within the material [15]:

Under light irradiation, h^+ in the valence band of WO_3 can participate in the oxidation of H_2O to generate •OH radicals, which are strong oxidizing agents capable of degrading organic pollutants. This is attributed to the oxidation potential of h^+ in the valence band of WO_3, which is approximately +3.4 V (vs. NHE), higher than the redox potential of the H_2O/•OH couple +2.8 V (vs. NHE). WO_3 can not only directly oxidize TNT via photogenerated h^+, but also indirectly contribute to the generation of •OH radicals from water, enhancing the degradation efficiency of TNT. This mechanism is consistent with previous studies [16].

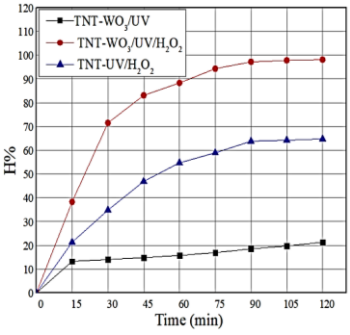

Figure 6. *TNT degradation performance of WO_3.*

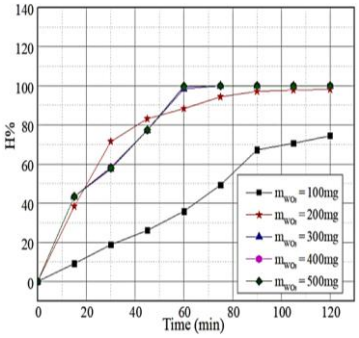

Figure 7. *Effect of WO_3 concentration on TNT degradation efficiency over time.*

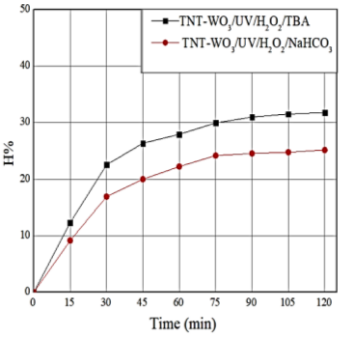

Figure 8. *TNT degradation using WO_3 in the presence of TBA and $NaHCO_3$.*

The addition of H_2O_2 significantly enhanced the TNT degradation efficiency. For the UV/H_2O_2 system, the optimal removal efficiency reached 63.8% after 120 minutes. When WO_3 was added as a photocatalyst, the UV/WO_3/H_2O_2 system achieved a much higher efficiency of 97.2% after 120 minutes. The presence of WO_3 contributed to the direct oxidation of TNT. The valence band h^+ of WO_3 possesses a more positive oxidation potential than the redox potential of the H_2O_2/•OH couple,

+1.49 V (vs. NHE), enabling it to indirectly participate in the oxidation of both $H_2O/•OH$ and $H_2O_2/•OH$ systems, thereby generating additional •OH radicals for enhanced TNT degradation [7].

Figure 7 illustrates the effect of WO_3 dosage on TNT degradation efficiency over time. As the WO_3 dosage increases from 100 to 500 mg, the treatment efficiency improves significantly. At WO_3 dosages of 100 mg and 200 mg, TNT degradation occurs more slowly, and complete removal is not achieved after 120 minutes. In contrast, dosages of 300, 400, and 500 mg yield nearly identical and complete degradation within 60–90 minutes. The dosage of 300 mg is considered optimal, providing high treatment efficiency while minimizing catalyst consumption. At this dosage, the degradation efficiency reached 98.7% within 60 minutes.

To validate and reinforce the experimental results, radical scavengers were introduced during the degradation process. The photocatalytic degradation of TNT using WO_3 was conducted under identical conditions in terms of catalyst dosage, TNT concentration, light intensity, and irradiation time, but in the presence of two different scavengers. The selected scavengers included TBA to quench •OH radicals, and $NaHCO_3$ to quench h^+.

The results presented in figure 8 show that the addition of TBA and $NaHCO_3$ led to a significant decrease in TNT degradation efficiency, with removal rates of 30.9% and 24.5% after 90 minutes, respectively. When TBA was introduced into the reaction system, •OH radicals rapidly reacted with TBA to form intermediate products, thereby reducing the amount of •OH available for TNT oxidation. The experimental results demonstrated a 66.3% reduction in TNT degradation efficiency, confirming that •OH radicals play a critical role in the $UV/WO_3/H_2O_2$ system [17]. Similarly, when $NaHCO_3$ was added, HCO_3^- ions captured photogenerated holes h^+, forming $CO_3•^-$ radicals, which possess lower oxidative activity. This process reduces the formation of •OH radicals, resulting in a 72.7% decrease in TNT degradation efficiency. This suggests that TNT may not only be oxidized by •OH radicals but also directly by h^+ on the surface of the WO_3 photocatalyst [18]. In addition, due to its low reduction potential, WO_3 is not capable of reducing O_2 to form superoxide radicals $O_2•^-$, •OH radicals and photogenerated h^+ are the primary reactive species in the $UV/WO_3/H_2O_2$. Comparison with other catalytic systems, such as UV-Fenton and TiO_2/UV shows that the $UV/WO_3/H_2O_2$ system offers higher removal efficiency and better operational stability under ambient temperature and low-pressure conditions [1, 4, 6].

3.3. Mechanism of TNT degradation by $UV/WO_3/H_2O_2$

The molecular structure of TNT consists of a CH_3^- attached at the 1-position and three NO_2^- located at the 2, 4, and 6 positions of the aromatic ring. The nitro groups are strong electron-withdrawing substituents, which decrease the electron density on the benzene ring and direct electrophilic attacks to the meta positions. Under mildly acidic conditions, pH from 4–5, the hydroxyl radical •OH acts as a powerful oxidizing agent, with a tendency to attack either the methyl group or the aromatic ring directly [19]. This process leads to the formation of intermediate products such as carboxylic acids and short-chain organic compounds. At the same time, the nitro groups may undergo oxidation or reduction, resulting in the release of NO_2^- and NO_3^- ions. The oxidation mechanism of TNT in the $UV/WO_3/H_2O_2$ system can be described as follows:

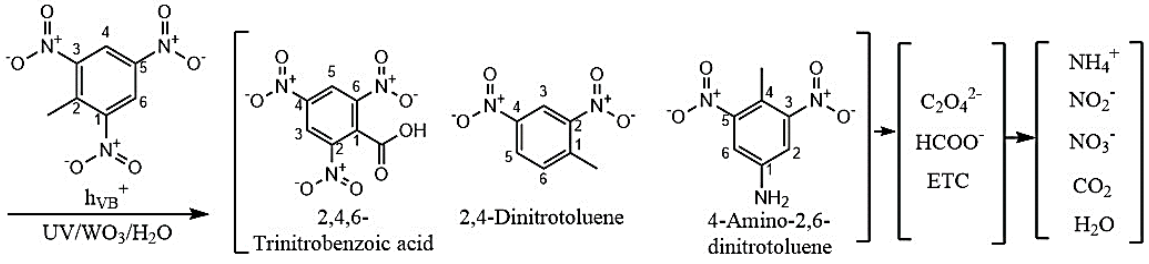

Figure 9. *TNT degradation mechanism of the $UV/WO_3/H_2O_2$ method.*

4. CONCLUSIONS

WO_3 material was successfully synthesized by the chemical precipitation method and applied in the UV/WO_3/H_2O_2 system for the treatment of TNT-contaminated wastewater. The synthesized material exhibited a hexagonal crystal structure, a band gap energy of approximately 3.3 eV, and strong absorption in the UV region. WO_3 demonstrated high stability and good photocatalytic activity under mildly acidic to neutral pH conditions. A catalyst dosage of 300 mg WO_3 combined with a fixed H_2O_2 concentration of 2.94×10^{-3} M was identified as the optimal condition, providing maximum TNT degradation efficiency. Under these parameters, the UV/WO_3/H_2O_2 system achieved a TNT degradation efficiency of 98.7% with an initial TNT concentration of 100 mg/L after 60 minutes of irradiation. The main oxidative species involved in the degradation process were identified as •OH and h^+, whose formation was attributed to the photocatalytic activity of WO_3. The synergistic effect of direct oxidation by h^+ and indirect oxidation via •OH, together with the ability to minimize sludge formation and operate efficiently over a wider pH range compared to conventional Fenton, UV/Fenton systems, highlights the potential of WO_3. However, as the material system tends to reach an energy equilibrium, the number of oxygen vacancies will gradually decrease over time. This study provides a foundation for the development of composite materials combining oxides with alkali or alkaline earth metals, aiming at catalysts that can be reused multiple times.

REFERENCES

[1]. Ayoub, K., et al. *"Application of advanced oxidation processes for TNT removal: A review"*, Journal of Hazardous Materials, 178(1–3), 10–28, (2010).

[2]. Ye, Z., Zhao, Q., et al. *"Acute toxicity evaluation of explosive wastewater by bacterial bioluminescence assays using a freshwater luminescent bacterium, Vibrio qinghaiensis sp. nov"*, Journal of Hazardous Materials, 186(2–3), 1351–1354, (2011).

[3]. Flokstra, B. R., et al. *"Microtox toxicity test: detoxification of TNT and RDX contaminated solutions by poplar tissue cultures"*, Chemosphere, 71(10), 1970–1976, (2008).

[4]. Zhang, Y., et al. *"Photocatalytic treatment of 2,4,6-trinitotoluene in red water by multi-doped TiO_2 with enhanced visible light photocatalytic activity"*, Colloids and Surfaces A: Physicochemical and Engineering Aspects, 452, 103–108, (2014).

[5]. Zhu, Q., Zhang, Y., et al. *"Cuprous oxide created on sepiolite: preparation, characterization, and photocatalytic activity in treatment of red water from 2,4,6-trinitrotoluene manufacturing"*, Journal of Hazardous Materials, 217–218, 11–18, (2012).

[6]. Bueno, P. R., et al. *"SnO_2, ZnO and related polycrystalline compound semiconductors: An overview and review on the voltage-dependent resistance (non-ohmic) feature"*, Journal of the European Ceramic Society, 28(3), 505–529, (2008).

[7]. Eroi, S. N., et al. *"Heterogeneous WO_3/H_2O_2 system for degradation of Indigo Carmin dye from aqueous solution"*, South African Journal of Chemical Engineering, 37, 53–60, (2021).

[8]. Chu, W., et al. *"Photocatalytic oxidation of monuron in the suspension of WO_3 under the irradiation of UV–visible light"*, Chemosphere, 86(11), 1079–1086, (2012).

[9]. Kolhe, P., et al. *"Facile hydrothermal synthesis of WO_3 nanoconifer thin film: multifunctional behavior for gas sensing and field emission applications"*, Journal of Inorganic and Organometallic Polymers and Materials, 29, (2019).

[10]. Tahir, M. B., et al. *"Nanostructured-based WO_3 photocatalysts: recent development, activity enhancement, perspectives and applications for wastewater treatment"*, International Journal of Environmental Science and Technology, 14(11), 2519–2542, (2017).

[11]. Muzaffar, T., et al. *"Synthesis and characterization of WO_3/GO nanocomposites for antimicrobial properties"*, Journal of Cluster Science, 33(5), 1987–1996, (2022).

[12]. Makuła, P., et al. *"How to correctly determine the band gap energy of modified semiconductor photocatalysts based on UV–Vis spectra"*, Journal of Physical Chemistry Letters, 9(23), 6814–6817, (2018).

[13]. Sánchez-Martínez, D., et al. *"Nanostructured-based WO_3 photocatalysts: recent development, activity enhancement, perspectives and applications for wastewater treatment"*, in: García-López, E. I., Palmisano, L. B. (Eds.), *Studies in Photocatalysis*, Elsevier, 211–220, (2021).

[14]. Jeyapaul, T., et al. *"Synthesis of WO_3 nanorods and their photocatalytic degradation of organic contaminants"*, Rasayan Journal of Chemistry, 11, 1405–1414, (2018).
[15]. Huo, N., et al. *"Synthesis of WO_3 nanostructures and their ultraviolet photoresponse properties"*, Journal of Materials Chemistry C, 1(25), 3999–4007, (2013).
[16]. Yan, M., et al. *"The fabrication of a novel Ag_3VO_4/WO_3 heterojunction with enhanced visible light efficiency in the photocatalytic degradation of TC"*, Physical Chemistry Chemical Physics, 18(4), 3308–3315, (2016).
[17]. Kouvelis, K., et al. *"Photocatalytic degradation of Losartan with BiOCl/sepiolite nanocomposites"*, Catalysts, 14, 433, (2024).
[18]. Fadaei, A., et al. *"Photocatalytic degradation of chlorpyrifos in water using titanium dioxide and zinc oxide"*, Fresenius Environmental Bulletin, 22(8), 2442–2447, (2013).
[19]. Augugliaro, V., et al. *"Overview on oxidation mechanisms of organic compounds by TiO_2 in heterogeneous photocatalysis"*, Journal of Photochemistry and Photobiology C: Photochemistry Reviews, 13(3), 224–245, (2012).

TÓM TẮT

Nghiên cứu khả năng xử lý trinitrotoluene trong nước bằng phương pháp quang oxi hóa UV/WO_3/H_2O_2

Bài báo trình bày kết quả tổng hợp vật liệu WO_3 bằng phương pháp kết tủa hóa học, cùng với việc đánh giá các tính chất hóa–lý, hình thái, cấu trúc tinh thể và đặc điểm hóa học của vật liệu. Ngoài ra, các kết quả sơ bộ cũng được giới thiệu về hiệu suất xử lý TNT trong nước bằng phương pháp quang oxy hóa, trong đó gốc hydroxyl •OH và h^+ đóng vai trò chính như là tác nhân oxy hóa chính. Kết quả cho thấy vật liệu WO_3 được tổng hợp có cấu trúc tinh thể lục giác, khối lượng riêng 7,920 g/cm³, cường độ hấp thụ 1,45 a.u tại bước sóng λ = 285 nm, và năng lượng vùng cấm đạt 3,3 eV. Quá trình proton hóa đã thúc đẩy mở rộng năng lượng vùng cấm và tăng cường thế oxy hóa của WO_3, từ đó cải thiện hiệu suất quang xúc tác và nâng cao khả năng hấp thụ ánh sáng UVB. Quá trình quang oxy hóa UV/WO_3/H_2O_2, với nồng độ H_2O_2 cố định 2,94 × 10^{-3} M, liều lượng xúc tác tối ưu 300 mg WO_3 và công suất đèn UV 10 W, đã đạt hiệu suất loại bỏ TNT 98,7% ở nồng độ ban đầu 100 mg/L sau 60 phút phản ứng ở điều kiện nhiệt độ môi trường.

Từ khóa: Vonfram trioxit; Quang oxy hóa; Trinitrotoluen; Xử lý.